

# Prediction of the tractor tire contact area, contact volume and rolling resistance using regression model and artificial neural network

Payam Farhadi<sup>1</sup>, Abdollah Golmohammadi<sup>1\*</sup>, Ahmad Sharifi<sup>2</sup>,  
Gholamhossein Shahgholi<sup>1</sup>

(1. *Department of Mechanics of Biosystem Engineering, University of Mohaghegh Ardabili, Ardabil, Iran;*

2. *Agricultural Engineering Research Institute, Agricultural Research, Education and Extension Organization (AREEO), Karaj, Iran)*

**Abstract:** A novel method to estimate the contact area and contact volume was developed with molding the tire footprint by liquid plaster and converting these molds to three-dimensional models using a 3D scanner. A 12.4-28, 6 ply tractor tire was operated under three levels of vertical load, three levels of inflation pressure and three levels of soil moisture content. To analyses the obtained data regression and artificial neural network (ANN) models were used and the accuracy of predicted results were compared with measured data. A multi-layer perceptron feed-forward ANN with back propagation (BP) learning algorithm was employed. Two hidden layers were used in network architecture and the best number of neuron for each hidden layer was selected with attention to minimum root mean square error (RMSE) criterion. The results showed that tire contact volume is a better parameter than tire contact area to predict rolling resistance. The comparison of the results of regression and ANN models to predict the contact area, contact volume and rolling resistance showed that ANN predictions had a closer agreement with the measured data than the regression model predictions.

**Keywords:** artificial neural network (ANN), contact area, contact volume, rolling resistance, three-dimensional footprint

**Citation:** Farhadi, P., A. Golmohammadi, A. Sharifi, and G. Shahgholi. 2019. Prediction of the tractor tire contact area, contact volume and rolling resistance using regression model and artificial neural network. *Agricultural Engineering International: CIGR Journal*, 21(3): 26–38.

## 1 Introduction

A tire is a ring-shaped vehicle component that covers the wheel's rim to protect it and enable better vehicle performance. Most tires provide through interaction between the vehicle and the terrain while providing a flexible cushion that absorbs shock. They also must perform functions such as supporting the weight of the vehicle, cushioning the vehicle over surface irregularities, providing sufficient traction for driving and braking, and providing adequate steering control and direction stability

(Wong, 2001). Since pneumatic tire do these tasks effectively, they are widely used in off-road vehicles and agricultural machines. Due to common use of these tires, many scientific studies have been performed on the interaction between the tire and the road surface. Tire-soil interaction in agricultural works is a very important subject because soil compaction, rolling resistance, loss of energy, and wheel slip are the result of soil - tire interactions (Taghavifar and Mardani, 2013a). Knowing that the power efficiency of pneumatic tires on concrete surfaces is about 90%, while it is sometimes less than 50% in loose or sandy soils, increases the importance of the issue and attention should be paid to fuel consumption (Gill and Vanden Berg, 1968; Wulfsohn et al., 1988).

Rolling resistance is defined as the difference between gross traction and net traction (ASABE, 2009) or the force resisting the motion when a wheel rolls on a

---

**Received date:** 2018-09-28    **Accepted date:** 2019-02-17

**\*Corresponding author:** Abdollah Golmohammadi, PhD, Associate Professor, Department of Mechanics of Biosystem Engineering, University of Mohaghegh Ardabili, Ardabil, Iran. Tel: 04515517500. Fax: 04515520567, Email: [agolmohammadi1342@gmail.com](mailto:agolmohammadi1342@gmail.com).

surface. It is mainly caused by non-elastic effects. Two forms of them are hysteresis losses in tire materials due to the deflection of the carcass while rolling, and permanent (plastic) deformation of the surface (e.g. soil surface). In the farmland in which deformation capacity of soil is greater than tire, rolling resistance force is greater due to the energy requirement for the soil deformation (Bygdén et al., 2004; Taghavifar and Mardani, 2013a).

Various parameters affect rolling resistance including tire load, tire inflation pressure, tire diameter, tire width, tire construction, tire tread, speed, surface adhesion, sliding, and relative micro-sliding between contact surfaces (Wong, 2001). Taghavifar and Mardani (2013a) studied the effect of inflation pressure, vertical load and velocity on rolling resistance for a small towed tire in a soil bin. Their obtained results showed that rolling resistance was a function of vertical load and tire inflation pressure and velocity was not significant. They also found that rolling resistance could be a function of contact area. Botta et al. (2012) studied the rolling resistance and soil compaction in agricultural traffic. They assessed the impact of two tractors with different tire sizes and axle loads on the motion resistance and the cone index for three different soil mechanical conditions. They also determine the existing relationships between motion resistance and ground pressure parameters and sinkage. In farmland that soil sinkage and soil deformation capability is high, it can be assumed that rolling resistance is a function of soil deformation. The contact area and contact volume is known as two criteria of soil deformation in tire-soil interaction, so various mathematical algorithms have been presented to predict tire contact area with the stiff ground (Grečenko, 1995) and many researchers have attempted to express the super ellipse shape of the tire surface in contact with the soil (Hallonborg, 1996; Keller, 2005; Roşca et al., 2014; Schjønning et al., 2015). In a number of studies image processing techniques was used to evaluate the effect of various tire-soil parameters on contact area (Diserens, 2009; Diserens et al., 2011; Taghavifar and Mardani, 2013a, 2013b). In image processing method after placing the tire on the ground, in order to distinguish between tire contact area and the non-contact surface of the soil, white powder is sprays around the tire and a photo is taken after

lifting the tire off the ground by a camera at a fixed distance and finally contact area is obtain by processing the photo in an image processing software. Low tire inflation pressure or high vertical load can lead to overloaded tires and soft surfaces, result in high sinkage (Hallonborg, 1996). Thus, due to sinkage in soft surface and the effect of tire-soil parameters on soil sinkage, it can be assume that contact volume is a better parameter than contact area for evaluating tire-soil interaction. In some studies the finite element method (FEM) was used for the analysis of tire-soil interaction (González Cueto et al., 2016; González Cueto et al., 2013), and in similar studies a combination of FEM for modelling tire and deeper layer of soil and the discrete element method (DEM) for modelling surface layer of soil were used (Michael et al., 2015; Nakashima and Oida, 2004). But in the field conditions, Mohsenimanesh and Ward (2010) estimated the 3D tire-soil footprint using dynamic contact pressures. They used six miniature pressure sensors, three on the tire lug surface and three on the region between two lugs. In their suggested method, maximum rut depth was considered to be coincident with the highest contact pressure and the sinkage of the other points were obtained according to the contact pressure ratio. So in their method, contact pressure was used as mediator parameter to estimate the depth of tire penetration on the soil, and the rut depth was not measured directly. Pierzchała et al. (2016) measured the wheel ruts and volume of the displaced soil using the close-range photogrammetry. Photogrammetry is the science of making measurements from photographs, especially for recovering the exact positions of surface points. In this study, they used an aerial image of wheel rutting. In order to calculate the volume of the displaced soil, they reconstructed the original terrain surface. Finally, they visually identified the surface that altered by the wheel rutting and clipped it from the surface model. The extraction trail model was compared with the pre-rutting terrain surface and using the software calculations, and thus the volume of soil deformation was obtained. Kenarsari et al. (2017) used the close-range digital photogrammetry to create 3D models of tractor tire footprints in the static and rolling condition of soil bin. They used the obtained models to estimate the tire footprint depth, area and volume. They

also evaluated the accuracy of the results obtained from this method and concluded that photogrammetry is a relatively strong technique in modelling the complex soil deformations in both static and rolling conditions. Also they concluded that lighting conditions are important especially for the dark organic soil.

Artificial neural networks (ANN) are widely applied to solve accidental and complex problems in a variety of science and engineering disciplines. The goal of the neural network is to solve problems in the same way that the human brain would. ANNs are able to learn incomplete data, deal with nonlinear problems and when trained, they can carry out predictions satisfactorily, also they have successfully been applied in the fields of pattern recognition, modelling, and control. Therefore, the use of ANN data analysis has increased in recent years. Alimardani et al. (2009) applied ANN model for prognostication of draft force and energy of subsoiling operation. They used three different algorithms for network training and finally due to higher accuracy of Levenberg-Marquardt (LM) algorithm than other algorithms, they used this algorithm. They also compared the accuracy of results from neural network models with the results obtained from the regression model and the advantages of neural network model to predict draft force and energy of subsoiling operation was concluded. Taghavifar et al. (2013c) applied a feed-forward ANN with back propagation (BP) learning algorithm and one hidden layer for estimation of tire rolling resistance by using input variables of vertical load, inflation pressure and velocity in clay-loam soil. Their results showed that the increasing of vertical load resulted in the increment of rolling resistance whereas the increase of inflation pressure had a reverse effect on rolling resistance. Taghavifar and Mardani (2014b) applied a supervised ANN method to prediction of driven tire energy efficiency indices. They used a feed-forward ANN with standard back propagation algorithm and two hidden layers to construct a supervised representation to predict the energy efficiency indices of driven wheels on a soil bin. The modelling performance revealed that ANN is a powerful technique to prediction of the stochastic energy efficiency indices. Thus, the aim of this study is measuring tire contact area and contact volume using a

unique method, and measuring the tire rolling resistance in various condition of vertical load, inflation pressure and soil moisture content in soil bin. Finally develop ANN and regression models to predict tire contact area and contact volume by using vertical load, inflation pressure and soil moisture also prognostication of rolling resistance by using contact area and contact volume as independent variables and compare the results of ANN and regression models.

## 2 Materials and methods

### 2.1 Tire test apparatus

A single wheel tester (SWT) was used for testing the tire in the soil bin (Figure 1). To supply tire motion power, a combination of 11 kW three-phase electric motor (model 160L4A; MOTOGEN Corporation., Tabriz, Iran) and gearbox with the reduction ratio of 1:104 was used to reduce the rotation velocity and increase the torque delivered to the tire. An alternating current (AC) motor speed controller (model LS600-2020; MAXTHERMO-GITTA Group Corp., New Taipei City, Taiwan) providing variable frequencies powered the electric motor, allowing the intended wheel rotational velocities to be attained. A torque transducer (Series 420 PTO system; PTO shaft torque and power system, Datum Electronics, East Cowes, United Kingdom) with a capacity of 1800 N m was installed between the electric motor and gearbox to measure torque, rotational velocity, and power delivered to the wheel. A hydraulic system with the output pressure of 1.5 MPa was used to provide vertical load on the tire. To power the hydraulic system, a 2.2 kW three-phase electric motor (model 112M6; MOTOGEN Co., Tabriz, Iran 2.2 kW; 112M6) with a gearbox was used. A compression load cell (model CLP-30KNB; Tokyo Sokki Kenkyujo Co., Ltd., Tokyo, Japan) with a 30 kN capacity was calibrated and then placed between hydraulic cylinder and frame to measure the vertical load on the tire. Also, a fifth wheel was mounted on the frame to measure the forward velocity using a digital encoder (model RS-58; RS Components Ltd., Corby, United Kingdom).

SWT was mounted on a soil bin in the laboratory of Iranian Agricultural Engineering Research Institute (AERI). The soil bin was 20 m long, 1.7 m wide, and

1.3 m deep, and filled with clay-loam soil. Soil textural composition and some mechanical characteristics are shown in Table 1. The soil is classified as CL-ML (i.e. an inorganic clay-loam soil with low plasticity) according to the Unified Soil Classification System (ASTM D 2487-83).

The experiments were conducted to investigate the effect of tire-soil interface on contact area, contact volume, and rolling resistance changes under different conditions of vertical load, inflation pressures, and soil moisture content with factorial layout at three replications by using of a Goodyear 12.4-28, 6 ply tractor tire. The soil bin is equipped with a soil processor system. Different levels of soil compaction can be achieved by adjusting the pressure of a compaction roller or the number of rolling passes on the soil layers. In preparing the soil for each test, the soil was added in 5 cm depth layer. After rolling the surface with a combination of a flat roller to compact the soil and a spike roller to lock the layers together, water was sprayed on the soil surface to achieve the desired moisture content. The tests were carried out in a certain range of soil moisture and according to the plastic limit of the soil. Accordingly, the soil with three moisture content of 0.46 PL (11.20% d.b.), 0.61 PL (14.86% d.b.) and 0.77 PL (18.68% d.b.) were prepared to perform the desired tests. Every layer was left for some minutes in order to allow the water to drain down and then the next layer was added. Tire rolling

resistance was measured in an approximately constant forward speed of 0.45 m s<sup>-1</sup>. A summary of the experimental dependent and independent variables is shown in Table 2. Regression models was achieved by using SPSS version 23 (IBM, Armonk, New York) statistical software.

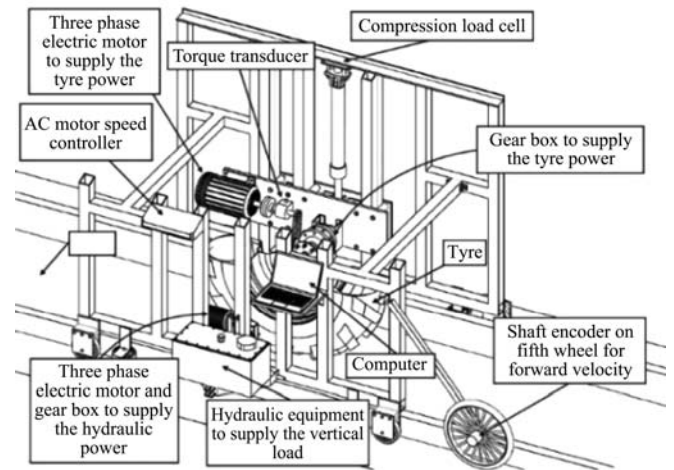


Figure 1 A schematic view of wheel tester and its components

**Table 1 Textural composition and some mechanical characteristics of the experimental soil**

	Characteristic	%
Textural composition	Clay	29
	Silt	33
	Sand	38
	Organic matter	1.7
	Organic carbon	0.6
Mechanical characteristics	Plastic limit (PL) moisture content	24
	Liquid limit (LL) moisture content	32
	Shrinkage limit (SL) moisture content	11

**Table 2 Summary of examined parameters**

Vertical load (kN)	Independent parameters					Soil moisture content (%d.b.)	Dependent parameters
	Inflation pressure (kPa)						
	Recommended inflation pressure (kPa) <sup>a</sup>	Actual inflation pressures used (kPa)					
6	32	80 (Overinflated)	120 (Overinflated)	160 (Overinflated)	11.20	Contact area	
9	109	80 (Underinflated)	120 (Overinflated)	160 (Overinflated)	14.86	Contact volume	
12	181	80 (Underinflated)	120 (Underinflated)	160 (Underinflated)	18.68	Rolling resistance	

Note: <sup>a</sup> For tire used as a single tire at a maximum speed of 40 km h<sup>-1</sup>. Source (Titan International, 2017).

**2.2 Tire contact area and contact volume measurement**

A new method was used to measure tire contact area, and the contact volume of soil deformation. At first, soil was prepared with the intended soil moisture content. Then, for every treatment, the tire with the intended vertical load and inflation pressure was placed on the soil. After a few seconds, the tire was removed from the soil. An example of tire footprint on soil is shown in Figure 2

(left). Because of the difficulty in the use of 3D scanner in soil bin and time saving, tire footprint on the soil was molded by liquid plaster and finally the mold was scanned together. At this stage, liquid plaster was used to mold the tire footprint. For this purpose, a sufficient amount of plaster mixed with water and finally liquid plaster was poured into the tire footprint (Figure 2, right). The liquid plaster covered the footprint with a 5 cm thick layer. The edge surface of footprint is known as the

non-deformation surface and considered as the reference plane. After the plaster dried, the dried plaster mold was removed from the soil and the extra soil was cleaned from the mold.



Figure 2 Tire footprint on the soil (left); molding of tire footprint with liquid plaster (right)

The obtained molds were converted to 3D models using a 3D scanner (model Rexcan 4; Solutionix Co., Seoul, Korea) (Figure 3, left). This scanner uses the phase-shifting optical triangulation technology and employs high resolution twin CCD cameras to achieve high-accuracy data. With the 3D model obtained from this method (Figure 3, right), we managed to extract information such as tire footprint volume and contact area relative to a reference plane.



Figure 3 Scanning a plaster mold samples using a 3D scanner (left); 3D model from scan (right)

The 3D models obtained from scan of plaster molds were analyzed by the Geomagic Studio 2014 SR3 software (3D Systems, Inc., Rock Hill, USA). Using this software and taking into consideration the soil surface as a reference plane, contact area, and soil deformation volume (footprint volume) were calculated. Equation (1) was used to calculate the tire contact area.

$$S = \sum_{i=1}^n S_i \tag{1}$$

where,  $S_i$ , is the resulted area at different portions of the contact surface ( $\text{cm}^2$ ) (Figure 4); and  $S$ , is the total contact area ( $\text{cm}^2$ ). Using a reference plane, the volume of soil deformation was considered as the volume that was placed at the top of the reference plane or under the undisturbed soil surface.

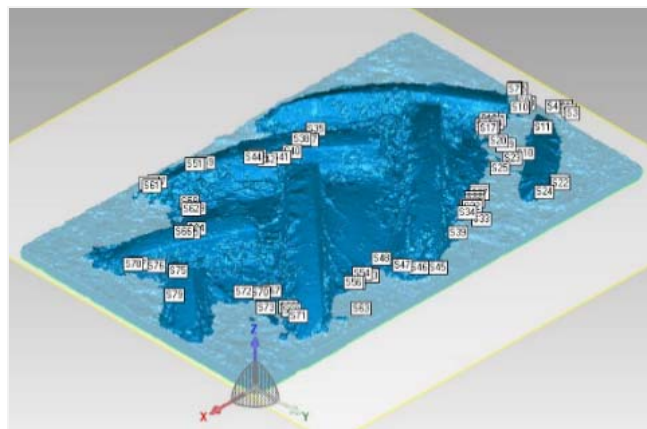


Figure 4 Reference plane with protrusion of the tire tread downward from the undisturbed soil surface shown inverted here, as upward protrusions. Numbers denote data points used in analysing the contact surface

### 2.3 Tire rolling resistance measurement

Based on Figure 5 the rolling resistance (also called motion resistance) of a wheel is equal to the difference between gross traction (GT) and net traction (NT) presented as follows (ASABE, 2009).

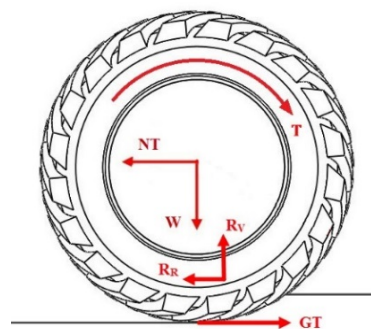


Figure 5 Basic forces on a wheel, including resultant soil reaction force

$$\text{Rolling Resistance (RR)} = \text{Gross Traction (GT)} - \text{Net Traction (NT)} \tag{2}$$

Part of the gross traction is required to overcome motion resistance which is the resistance to the movement of the wheel through the soil and the remainder is equal to net traction. In this study, net traction value applied to the single wheel tester was zero, therefore the tire rolling resistance force can be calculated by measuring the electric motor torque. Electric motor torque measured data from the torque transducer using TorqueLog 1.6 software (Datum Electronics, Ltd., East Cowes, United Kingdom) was stored on the computer in the Microsoft Excel spreadsheet format. Rolling resistance was measured at the distance of approximately 4 m for each treatment. To obtain the rolling resistance force, the Equation (3) was used.

$$R_r = \frac{EMT \times 104 \times GE}{R} \quad (3)$$

where,  $R_r$ , is rolling resistance force (N);  $EMT$  (electromotor torque), is measured torque from the torque transducer (N m); 104, is gearbox reduction ratio;  $GE$ , is gearbox efficiency and;  $R$ , is rolling radius of the tire at zero condition (m) (ASABE, 2009). At the start of the tire movement, the force applied to the tire showed variable values, but after a few seconds, its value became relatively stable (Figure 6). To analysis of the data, the mean value of rolling resistance in the stable region was used.

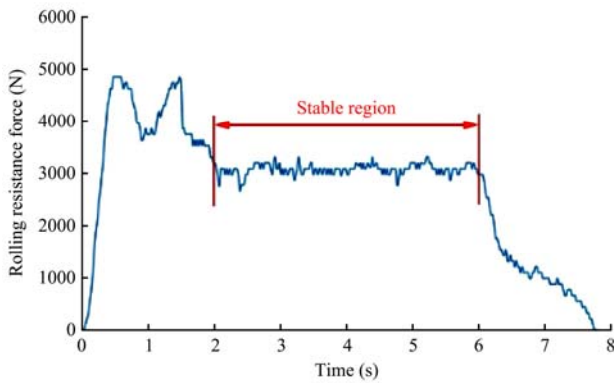


Figure 6 An example of the graph obtained for rolling resistance and stable region

## 2.4 ANN development

In this study two separate ANN algorithm in order to predict the intended parameters were used (detailed in Table 3). MATLAB R2014b software (Math Works, Inc., Natick, Mass., USA) was used to develop ANN models. Input data of variables were randomly divided and shuffled into three different sets for training, cross-validation and testing the neural networks. In training step the network is adjusted according to its error and in validation step data used to measure network generalization and to halt training when generalization stops improving and finally in testing step that have no effect on training and so provide an independent measure of network performance during and after training. In training, validation, and testing step, 70%, 15%, and 15% portions of input variables were considered respectively. For regression models, variables were divided into two portions 70% and 30% for training and testing step. In the field of data analysis, the best results are often obtained by a multilayer perceptron (MLP) with back BP algorithm (Jevšenak and Levanič, 2016), therefore a

feed-forward ANN with BP algorithm was employed. **trainlm** training function that updates weight and bias values based on the LM and often considered as the fastest BP algorithm and highly recommended as a first-choice supervised algorithm, was used (MATLAB, 2014). Since increasing number of hidden layers may increase efficiency of the system (Taghavifar and Mardani, 2014b), therefore two hidden layers was assumed for implementations. In the other hand, for determination number of neuron in each hidden layer ( $N_1$  and  $N_2$ ) the number of neurons in hidden layers were increased from 1 to 10. Finally for selecting of appropriate structure of network two criteria of Root Mean Square Error (RMSE) and  $R^2$  was used (Equation (4) and (5)).

Table 3 Summary of ANN Algorithm structures

Network number	Input (s)	Unit	Output (s)	Unit	Algorithm structure
1	Load	kN	Contact area	cm <sup>2</sup>	3-N <sub>1</sub> -N <sub>2</sub> -2
	Inflation	kPa			
	Soil moisture content	%d.b	Contact volume	cm <sup>3</sup>	
2	Contact volume	cm <sup>3</sup>	Rolling resistance	kN	1-N <sub>1</sub> -N <sub>2</sub> -1

In every two hidden layers of network tangent sigmoid (*transig*) transfer function and in the output layer a linear transfer function (*purelin*) was used. *Transig* transfer function generates values in the range of  $-1$  to  $1$ , and *purelin* transfer function produces results in the range of  $-\infty$  to  $+\infty$ .

$$RMSE = \sqrt{\frac{1}{n} \sum_{i=1}^n (Y_{predicted} - Y_{measured})^2} \quad (4)$$

$$R^2 = \frac{\sum_{I=1}^N (Y_{predicted} - Y_{measured})^2}{\sum_{I=1}^N (Y_{predicted} - Y_{mean})^2} \quad (5)$$

where,  $Y_{measured}$  and  $Y_{predicted}$  are measured and predicted values by the developed models, respectively. To achieve fast convergence to minimal RMSE, the input variables was normalized in the range of  $-1$  to  $1$  due to deference in input variables range by using of Equation (6) (Taghavifar and Mardani, 2014a).

$$X_n = 2 \frac{X_r - X_{r,\min}}{X_{r,\max} - X_{r,\min}} - 1 \quad (6)$$

where,  $X_n$ , is normalized input variable;  $X_r$ , is the raw input variable; and  $X_{r,\min}$ , and  $X_{r,\max}$ , define the minimum and maximum of the input variable.

### 3 Results and discussion

#### 3.1 Effect of vertical load, inflation pressure, and soil moisture content on contact area and contact volume

The 3D models obtained from scanning of plaster molds were analyzed by the Geomagic Studio 2014 SR3 software. Obtained value of contact area and contact volume from analysis of 3D scanned mold were shown in Figure 7. Results showed that minimum and maximum contact areas were achieved in the soil moisture levels of 11.20% and 18.68% d.b., and for the treatments of 6 kN-160 kPa and 12 kN-80 kPa, respectively. It can be seen that by increasing the soil moisture content, the tire contact area was increased. Such trends in increasing contact area were also been mentioned in other experimental studies (Wong, 2001). Also at each soil moisture level, with increasing the vertical load at constant inflation pressure, the tire contact area was increased, which agree with the results reported by other researchers (Mohsenimanesh and Ward, 2010; Taghavifar and Mardani, 2013a, 2013b). In each soil moisture level for constant vertical load, with increasing the inflation pressure, the tire contact area was decreased. Such results have been obtained by other experimental studies (Diserens, 2009; Schjøning et al., 2008; Taghavifar and Mardani, 2013b). Wong (2001) mentioned that with increasing soil moisture content, the rut depth become deeper, and in current study by increasing the soil moisture content, rut depth and afterward tire contact volume was increased (Figure 7). In the other hand at

each level of soil moisture content, by increasing the vertical load at constant inflation pressure, the contact volume was increased, which is consistent with previous research results (Mohsenimanesh and Ward, 2010). Therefore maximum and minimum values of contact volume were achieved at soil moisture contents of 18.68% and 11.20% d.b., respectively. Mohsenimanesh and Ward (2010) reported that inflation pressure had a reverse effect on tire contact volume, while in this experiment it was confirmed that the increment of inflation pressure increased soil sinkage and finally tire contact volume. Several researchers (Bygdén et al., 2004; Kurjenluoma et al., 2009) referred that vertical load and inflation pressure had a significant effect on rut depth, and in the current study, effect of rut depth increment on increasing the contact volume with increasing vertical load, inflation pressure and soil moisture content approved (Figure 7).

Figure 8 showed the tire contact area and tire contact volume changes versus tested variables of inflation pressure, vertical load and soil moisture content for all examined treatments.

Based on Figure 8 the quadratic relationship between tire contact area and tire contact volume with all tested parameters are shown, so it seems more reasonable to describe their relation as a second order regression equation. The variables of vertical load, inflation pressure and soil moisture content were used to predict the contact area and contact volume by using multiple regression and ANN models.

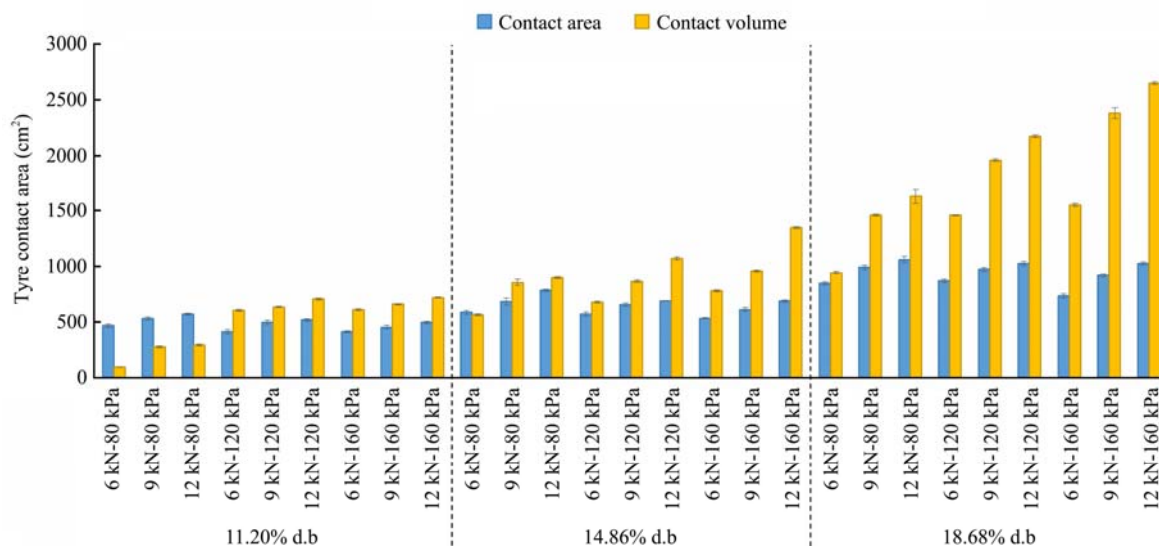


Figure 7 Contact area and contact volume changes for all examined treatment

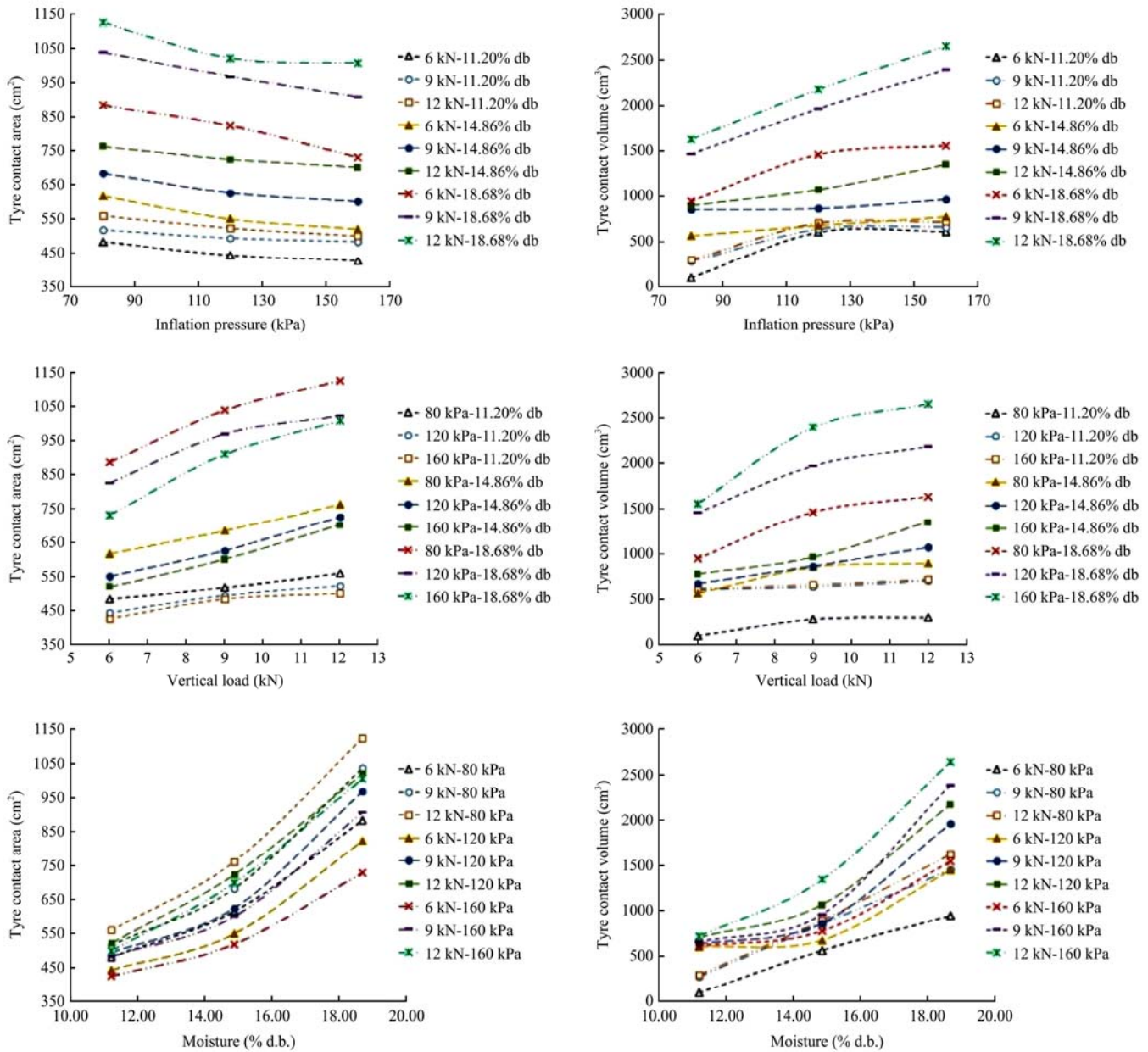


Figure 8 Tyre contact area and tire contact volume changes versus input variables for all treatments

The multiple regression resulting models to predict the contact area and contact volume based on 70% of data are shown in Equation (7) and (8), respectively. The adjusted R square value of 0.974 and 0.922 achieved for contact area and contact volume in testing step respectively.

$$CA = -2.168L^2 + 65.443L - 0.001P^2 - 0.702P + 4.508M^2 - 73.962M + 443.234 \quad (7)$$

$$CA = -8.275L^2 + 226.858L - 0.057P^2 + 20.093P - 18.108M^2 - 368.459M - 488.666 \quad (8)$$

where,  $CA$ , is contact area ( $cm^2$ );  $CV$ , is contact volume ( $cm^3$ );  $L$ , is vertical load on tire (kN);  $P$ , is tire inflation pressure (kPa); and  $M$ , is soil moisture content (% d.b.). The resulting regression function for contact area has a

weak relation with variables of inflation pressure that agree with previous obtained results (Taghavifar and Mardani, 2013b), but the obtained model for contact volume has a greater relation with variable of inflation pressure that shows the effect of this parameter on soil sinkage (Bygdén et al., 2004; Kurjenluoma et al., 2009) and finally tire contact volume.

A neural network with three variables of vertical load, inflation pressure and soil moisture content in the input layer and variables of contact area and contact volume in the output layer was created. Also two hidden layers was used for creating neural network structure. To select the number of neurons in each hidden layer ( $N_1$  and  $N_2$ ), the RMSE criterion was used. Figure 9 shows the RMSE

changes against the number of neurons in each hidden layer. Based on the lowest RMSE value, the best number of neuron for first and second hidden layer was achieved in 4 and 8, respectively. It can be seen that, the low number of neurons in each hidden layer, increases the RMSE value, so that the highest value of the RMSE was achieved in 9 and 1 respectively for  $N_1$  and  $N_2$ . The correlation coefficient for the training, validation and testing were 0.999, 0.997 and 0.999 respectively.

Distribution of predicted values versus measured values obtained by regression and ANN models for dependent variables of contact area and contact volume was shown in Figure 10. The  $R$  square values of 0.967 and 0.979 was achieved for all data by using ANN model to contact area and contact volume respectively based on variables of vertical load, inflation pressure and soil moisture content. With attention to Figure 10, it can be seen that ANN model has a closer predicted data to actual data in comparison with the regression models.

Figure 11 and Figure 12 shows a comparison between measured and predicted value by using regression and ANN models for all treatments. With attention to these figures it can be seen that ANN model has a performance better than regression model that mentioned by Jevšenak and Levanič (2016).

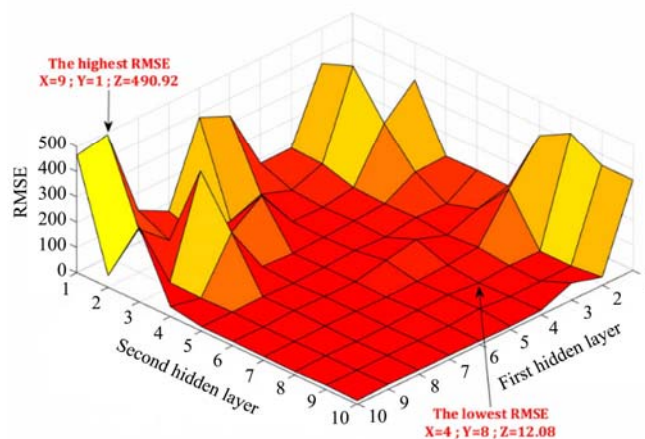


Figure 9 Changes of RMSE versus changes on number of neuron in each hidden layer for parameters of contact area and contact volume network

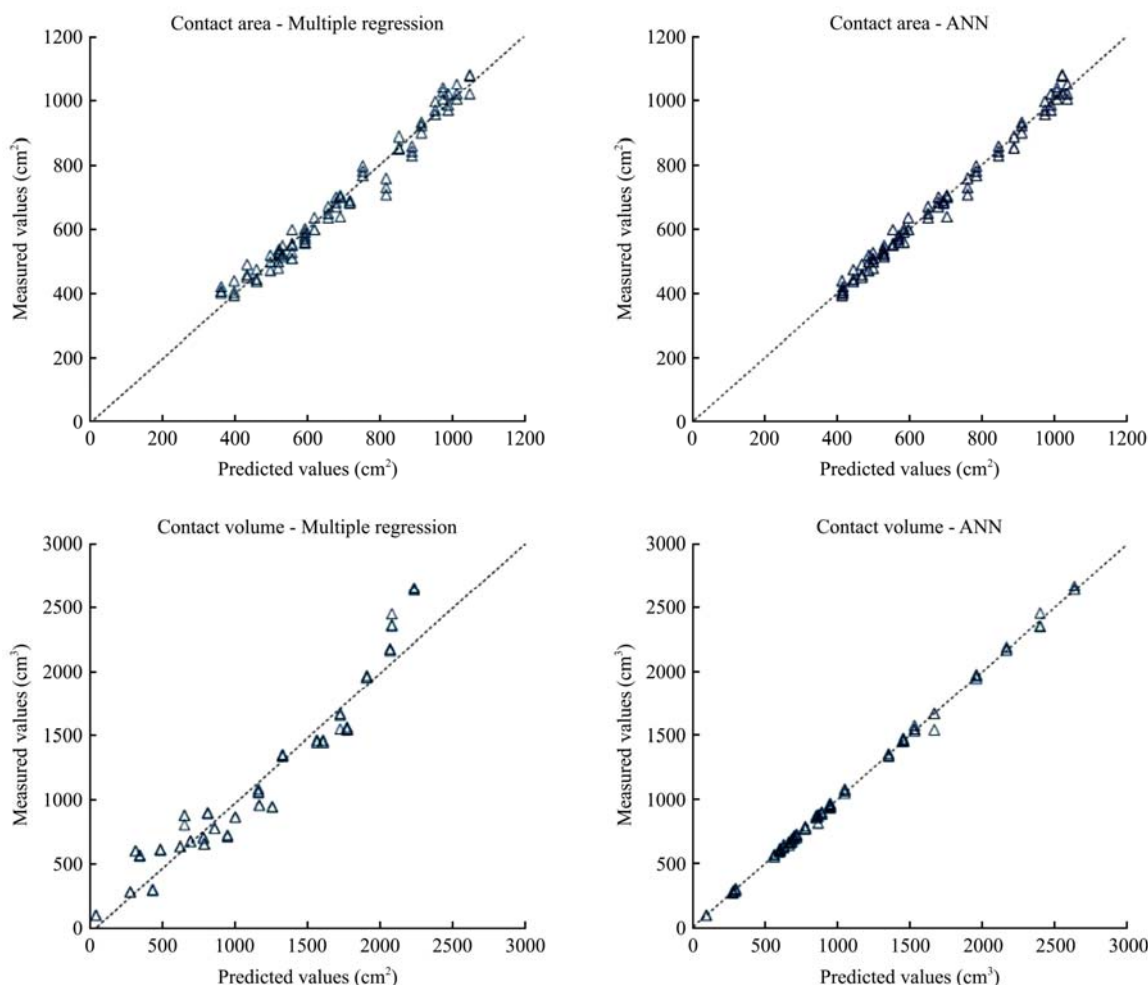


Figure 10 Distribution of predicted values versus measured values obtained by regression and ANN models

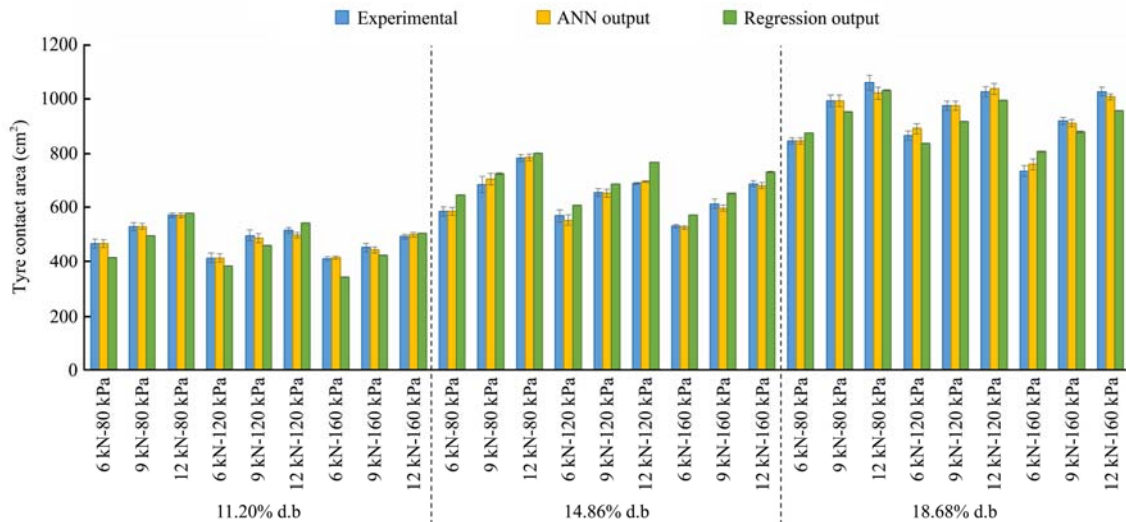


Figure 11 Comparison between measured and predicted values of contact area by using of regression and ANN models

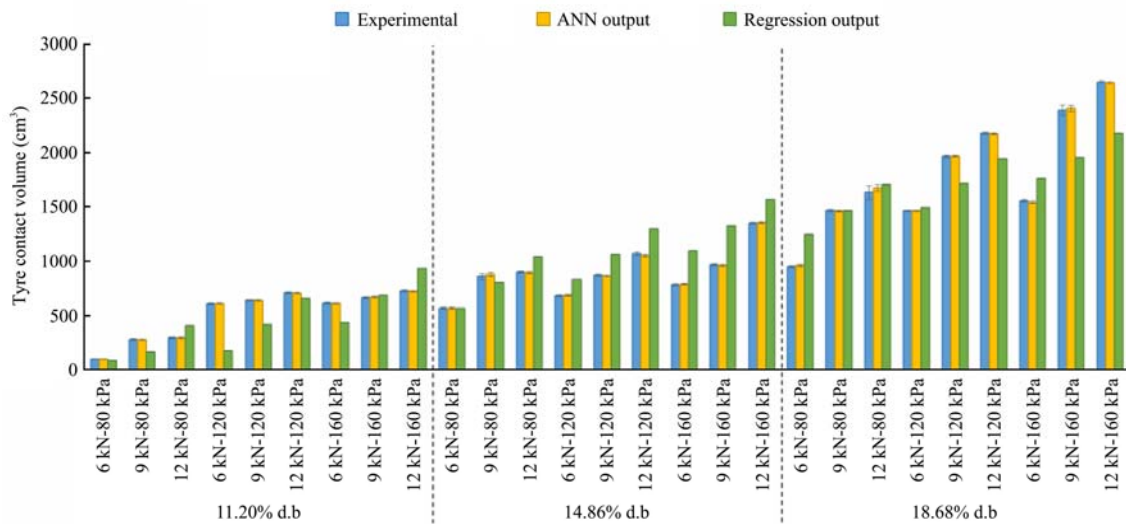


Figure 12 Comparison between measured and predicted values of contact volume by using of regression and ANN models

**3.2 Effect of contact volume on rolling resistance**

The impact of vertical load and tire inflation pressure on the accelerated growth of tire rolling resistance was obvious at the soil moisture content of 14.86% and 18.68% d.b., due to the increment of soil sinkage and tire contact volume. Variables of vertical load, tire inflation pressure, and soil moisture content affect contact area, contact volume and subsequently tire rolling resistance. Therefore, it can be assumed that rolling resistance is a function of tire contact area and tire contact volume. So two separate univariate regression model were used to obtain the relationship between the parameters of rolling resistance with tire contact area and tire contact volume. Bygdén et al. (2004) have considered reducing the rut deformation as a major factor in reducing rolling resistance. In the other hand due to vertical soil deformation or volume

deformation, contact volume could be consider as a better parameter than contact area for estimating the rolling resistance. The resulting regression model is based on 70% of data to predict rolling resistance with contact area and contact volume is presented in Equation (9) and (10) respectively. The adjusted *R* square value of 0.613 and 0.933 were achieved for contact area and contact volume based equation to predict of rolling resistance.

$$R_R = 3.062CA + 1394.268 \tag{9}$$

$$R_R = 1.253CV + 2304.136 \tag{10}$$

To estimate rolling resistance based on contact volume, a neural network with variable of contact volume in the input layer and rolling resistance in output layer and two hidden layers were used for creating neural network structure. In this network to determine the number of neurons in the first and second hidden layers

the RMSE criterion was used and the best number of neuron for  $N_1$  and  $N_2$  was achieved 7 and 9 respectively in the minimum value of RMSE (Figure 13). The correlation coefficient for the training, validation and testing were 0.991, 0.826 and 0.945 respectively.

Scatterplot of predicted values versus measured values obtained by regression and ANN models for rolling resistance are shown in Figure 14. The  $R$  square values of 0.960 was achieved for all rolling resistance data by using ANN model that was a little more than the value obtained using regression model ( $R^2=0.933$ ). The comparison of ANN model and regression model to predict the rolling resistance shows that ANN data were more close to actual data than the regression model

(Alimardani et al., 2009) that could be seen in Figure 14 and 15.

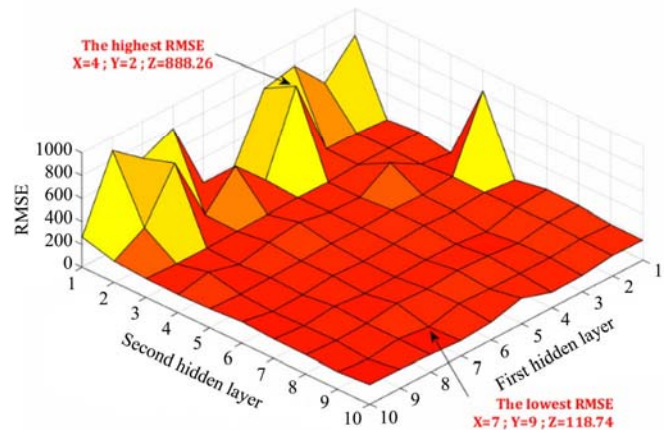


Figure 13 Changes of RMSE versus changes on number of neuron in each hidden layer for rolling resistance network

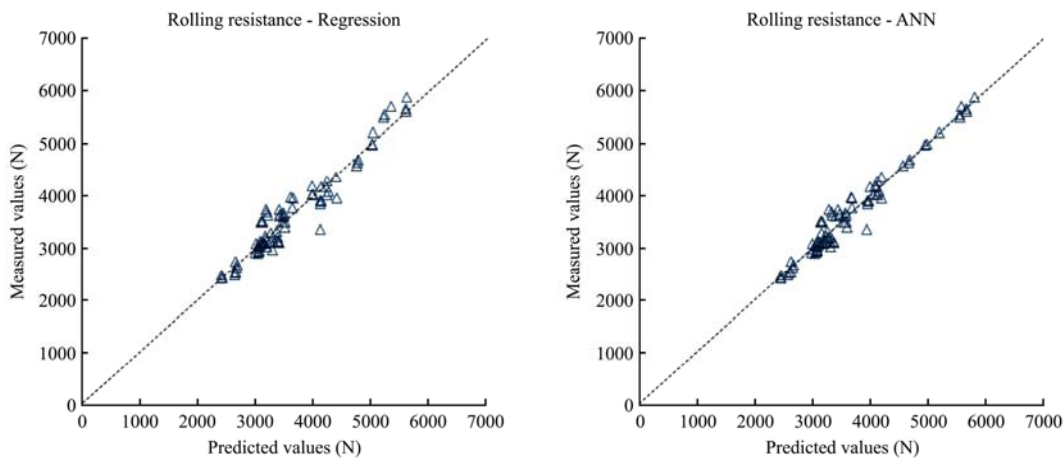


Figure 14 Distribution of rolling resistance predicted values versus measured values obtained by regression and ANN models based on contact volume

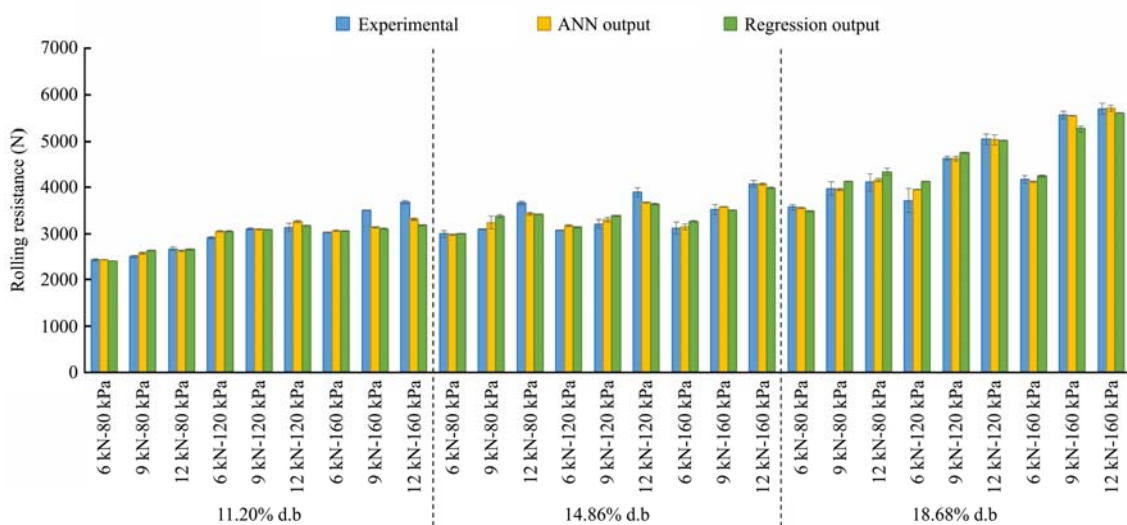


Figure 15 Comparison between measured and predicted values of rolling resistance by using of regression and ANN models

Rolling resistance variation versus the change of vertical load and inflation pressure parameters for three soil moisture content levels are shown in Figure 15. It can be seen that increasing of vertical load and soil moisture

content increases rolling resistance. Increasing of inflation pressure causes in increase of rolling resistance that decline obtained results by Taghavifar et al. (2013c) because by increasing inflation pressure, tire contact

volume and energy expended to soil deformation that the main reason to create rolling resistance (Wong, 2001) was increased.

#### 4 Conclusions

In this study a unique method based on molding the tire footprint by liquid plaster and converting these molds to three-dimensional models using a 3D scanner was used. This method lacks the disadvantage of estimating the area of the tire footprint due to the difficulty of manually setting the boundary of the footprint. The detection of the contact area between the tire and the soil is performed by defining and using a reference plane. Another advantage of this method is the possibility of point-to-point comparison of 3D footprint models for two different operating conditions. Linear regression and ANN methods to investigate the tire-soil parameters on contact area and contact volume also prediction of rolling resistance by using contact area and contact volume were used and the following conclusions were obtained. By increasing the vertical load and soil moisture content, contact area and contact volume parameters were increased and by increasing the inflation pressure, contact area decreased and contact volume increased. The regression analyses of contact area and contact volume revealed a high correlation with vertical load, inflation pressure, and soil moisture content ( $R^2= 0.974$  and  $0.922$  respectively). Also rolling resistance showed a high correlation with contact volume ( $R^2= 0.933$ ) that shows the rolling resistance as a dependent variable of tire contact volume. Generally increment of neuron numbers leads to reduction of RMSE in all analyses. Increasing in number of neurons increases quality of network modelling, however, enhances complexity of the developed network. ANN models predicted values were very close to measured data compared to results obtained from linear regression models. So it can be concluded that ANN could be a more effective method than regression models, which produces better results and can be properly used for rolling resistance prediction.

#### Acknowledgements

The authors would like to thank the staff of Soil Bin Laboratory, Mr. Hossein Seraje, Mr. Naghi Mohebbi and

Mr. Mehdi Naziri, Iranian Agricultural Engineering Research Institute (AERI), for their efforts to conduct this study.

#### References

- Alimardani, R., Y. Abbaspour-Gilandeh, A. Khalilian, A. Keyhani, and S. H. Sadati. 2009. Prediction of draft force and energy of subsoiling operation using ANN model. *Journal of Food, Agriculture & Environment (JFAE)*, 7(3&4): 537–542.
- ASABE Standards. 2009. ANSI/ASAE S296.5 DEC2003(R2009). General terminology for traction of agricultural traction and transport devices and vehicles. St. Joseph, Mich. USA: ASABE.
- ASTM Standards. 1985. ASTM D2487-83. Classification of soils for engineering purposes. West Conshohocken, PA: ASTM International.
- Botta, G. F., A. Tolon-Becerra, M. Tourn, X. Lastra-Bravo, and D. Rivero. 2012. Agricultural traffic: Motion resistance and soil compaction in relation to tractor design and different soil conditions. *Soil and Tillage Research*, 120: 92–98.
- Bygdén, G., L. Eliasson, and I. Wästerlund. 2004. Rut depth, soil compaction and rolling resistance when using bogie tracks. *Journal of Terramechanics*, 40(3): 179–190.
- Diserens, E. 2009. Calculating the contact area of trailer tyres in the field. *Soil and Tillage Research*, 103(3): 302–309.
- Diserens, E., P. Défossez, A. Duboisset, and A. Alaoui. 2011. Prediction of the contact area of agricultural traction tyres on firm soil. *Biosystems Engineering*, 110(2): 73–82.
- Gill, W. R., and G. E. Vanden Berg. 1968. Soil dynamics in tillage and traction. Washington, D. C.: Agricultural Research Service, US Department of Agriculture.
- González, O., C. E. Iglesias Coronel, E. López, C. A. Recarey, and M. Herrera. 2016. Modelling in FEM the soil pressures distribution caused by a tyre on a Rhodic Ferralsol soil. *Journal of Terramechanics*, 63: 61–67.
- González, O., C. E. Iglesias, C. A. Recarey, G. Urriolagoitia, L. H. Hernández, G. Urriolagoitia, and M. Herrera. 2013. Three dimensional finite element model of soil compaction caused by agricultural tire traffic. *Computers and Electronics in Agriculture*, 99: 146–152.
- Grečenko, A. 1995. Tyre footprint area on hard ground computed from catalogue values. *Journal of Terramechanics*, 32(6): 325–333.
- Hallonborg, U. 1996. Super ellipse as tyre-ground contact area. *Journal of Terramechanics*, 33(3): 125–132.
- Jevšenak, J., and T. Levanič. 2016. Should artificial neural networks replace linear models in tree ring based climate reconstructions? *Dendrochronologia*, 40: 102–109.
- Keller, T. 2005. A model for the prediction of the contact area and the distribution of vertical stress below agricultural tyres from

- readily available tyre parameters. *Biosystems Engineering*, 92(1): 85–96.
- Kenarsari, A. E., S. J. Vitton, and J. E. Beard. 2017. Creating 3D models of tractor tire footprints using close-range digital photogrammetry. *Journal of Terramechanics*, 74: 1–11.
- Kurjenluoma, J., L. Alakukku, and J. Ahokas. 2009. Rolling resistance and rut formation by implement tyres on tilled clay soil. *Journal of Terramechanics*, 46(6): 267–275.
- MathWorks. Artificial neural network toolbox user's guide, for the use of Matlab. The Math Works Inc; 2014. Available at: [www.mathworks.com](http://www.mathworks.com). Accessed 10 June 2018.
- Michael, M., F. Vogel, and B. Peters. 2015. DEM–FEM coupling simulations of the interactions between a tire tread and granular terrain. *Computer Methods in Applied Mechanics and Engineering*, 289: 227–248.
- Mohsenimanesh, A., and S. M. Ward. 2010. Estimation of a three-dimensional tyre footprint using dynamic soil–tyre contact pressures. *Journal of Terramechanics*, 47(6): 415–421.
- Nakashima, H., and A. Oida. 2004. Algorithm and implementation of soil–tire contact analysis code based on dynamic FE–DE method. *Journal of Terramechanics*, 41(2-3): 127–137.
- Pierzchała, M., B. Talbot, and R. Astrup. 2016. Measuring wheel ruts with close-range photogrammetry. *Forestry: An International Journal of Forest Research*, 89(4): 383–391.
- Roşca, R., P. Cârlescu, I. Țenu. 2014. A semi-empirical traction prediction model for an agricultural tyre, based on the super ellipse shape of the contact surface. *Soil and Tillage Research*, 141: 10–18.
- Schjønning, P., M. Lamandé, F. A. Tøgersen, J. Arvidsson, and T. Keller. 2008. Modelling effects of tyre inflation pressure on the stress distribution near the soil–tyre interface. *Biosystems Engineering*, 99(1): 119–133.
- Schjønning, P., M. Stettler, T. Keller, P. Lassen, and M. Lamandé. 2015. Predicted tyre–soil interface area and vertical stress distribution based on loading characteristics. *Soil and Tillage Research*, 152: 52–66.
- Taghavifar, H., and A. Mardani. 2013a. Investigating the effect of velocity, inflation pressure, and vertical load on rolling resistance of a radial ply tire. *Journal of Terramechanics*, 50(2): 99–106.
- Taghavifar, H., and A. Mardani. 2013b. Potential of functional image processing technique for the measurements of contact area and contact pressure of a radial ply tire in a soil bin testing facility. *Measurement*, 46(10): 4038–4044.
- Taghavifar, H., and A. Mardani. 2014a. Application of artificial neural networks for the prediction of traction performance parameters. *Journal of the Saudi Society of Agricultural Sciences*, 13(1): 35–43.
- Taghavifar, H., and A. Mardani. 2014b. Applying a supervised ANN (artificial neural network) approach to the prognostication of driven wheel energy efficiency indices. *Energy*, 68: 651–657.
- Taghavifar, H., A. Mardani, H. Karim-Maslak, H. Kalbkhani. 2013c. Artificial Neural Network estimation of wheel rolling resistance in clay loam soil. *Applied Soft Computing*, 13(8): 3544–3551.
- Titan International. 2017. Goodyear Tires. Available at: <http://tiregroup.com/wp-content/themes/tiregroup/pdf/titan-ag-tires.pdf>. Accessed 15 November 2015.
- Wong, J. Y. 2001. *Theory of Ground Vehicles*. 3rd ed. New York: John Wiley & Sons, Inc..
- Wulfsohn, D., S. K. Upadhyaya, and W. J. Chancellor. 1988. Tractive characteristics of radial ply and bias ply tyres in a California soil. *Journal of Terramechanics*, 25(2): 111–134.